Molecular Crystals and Liquid Crystals Science and Technology. Section A. Molecular Crystals and Liquid Crystals

Publication details, including instructions for authors and subscription information:
http://www.tandfonline.com/loi/gmcl19

New Chiral Series with Large Tilt Angle in the Ferroelectric Smectic Phase

P. Cluzeau [a], M. Ismaili [a], A. Anakkar [a], M. Foulon [a], A. Babeau [b] & H. T. Nguyen [b]

[a] Laboratoire de Dynamique et Structure des matériaux Moléculaires, UPRESA CNRS 8024, Bâtiment P5, Université de Lille I, 59655, Villeneuve d'Ascq, France

[b] Centre de Recherche Paul Pascal, CNRS, Avenue A. Schweitzer, 33600, Pessac, France

Version of record first published: 24 Sep 2006

To cite this article: P. Cluzeau, M. Ismaili, A. Anakkar, M. Foulon, A. Babeau & H. T. Nguyen (2001): New Chiral Series with Large Tilt Angle in the Ferroelectric Smectic Phase, Molecular Crystals and Liquid Crystals Science and Technology. Section A. Molecular Crystals and Liquid Crystals, 362:1, 185-202

To link to this article: http://dx.doi.org/10.1080/10587250108025769

Mol. Cryst. Liq. Cryst., Vol. 362, pp. 185-202
Reprints available directly from the publisher
Photocopying permitted by license only

New Chiral Series with Large Tilt Angle in the Ferroelectric Smectic Phase

P. CLUZEAU[a*], M. ISMAILI[a], A. ANAKKAR[a], M. FOULON[a], A. BABEAU[b] and H. T. NGUYEN[b]

[a]Laboratoire de Dynamique et Structure des matériaux Moléculaires, UPRESA CNRS 8024, Bâtiment P5, Université de Lille I, 59655 Villeneuve d'Ascq, France and [b]Centre de Recherche Paul Pascal, CNRS, Avenue A. Schweitzer, 33600 Pessac, France

A new series of chiral homologous thiobenzoates with aliphatic end chains ranging from heptyloxy to dodecyloxy has been synthesized. It has been characterized by optical microscopy, DSC, pitch measurements and electro-optical study. The typical phase sequence of this series on heating is SmC^*, N^*, BPI, BPII and I phases. The interesting feature of these compounds is to exhibit the SmC^*-N^* phase transition; moreover the tilt angle in the ferroelectric smectic phase is very large (~ 45°) and quasi-temperature independent.

Keywords: ferroelectric liquid crystal; large tilt angle

I INTRODUCTION

Despide of the recent discovery of a new class of ferroelectric liquid crystals built up with achiral polyphilic molecules [1] or recently, banana-shape molecules [2]; conventional ferroelectric liquid crystals remain of a considerable theoretical and technological interest [3].

This paper presents a detailed analysis of a new chiral series derived from 4-alkoxy-4′-mercaptobiphenyl. All the compounds of this series (in short nBSMHOB; n varies from 7 to 12) exhibit the SmC^*-N^* phase transition. The molecular tilt angle θ in the SmC^* phase displays high values up to 45° and is quasi-temperature independent.

These compounds are convenient to study critical phenomena at the SmC^*-N^* phase transition on free standing film [4]. Moreover, owing to the tilt angle value of 45°, this series is potentially interesting to realize electrooptical device with a

* Corresponding author.

high capability of producing grey-scale. These ferroelectric liquid crystal light modulators are known as "Twisted Smectic C*" (TSC) liquid crystal cells or Patel cells [5]. The experimental studies of free standing films and of Patel cells are the main aims of the present characterization study.

II SYNTHESIS

The studied materials were prepared by esterification reaction between the chiral 4-alkyloxybenzoic acid and the corresponding 4-alkyloxy-4′-mercaptobiphenyl following the scheme 1.

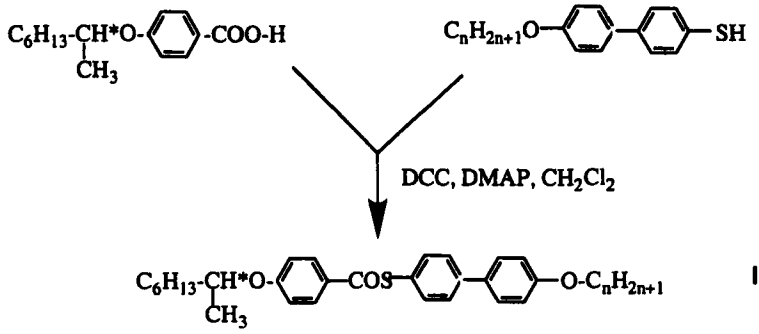

SCHEME 1 S-4-alkyloxybiphenylyl (S)-4-(1-methylheptyloxy)benzoates

The chiral benzoic acid was synthesized following the scheme 2:

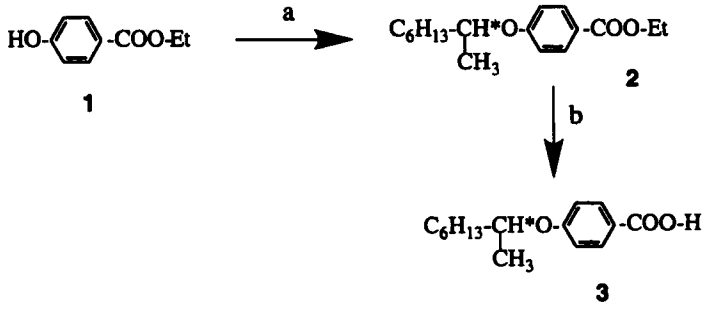

a) (R)-2-octanol, DEAD, Ph_3P, CH_2Cl_2

b) KOH, EtOH then acid hydrolysis

SCHEME 2 Synthesis of (S)-4-(1-methylheptyloxy)benzoic acid

The 4-alkyloxy-4′-mercaptobiphenyl is obtained with the Montéro's method [6] (scheme 3)

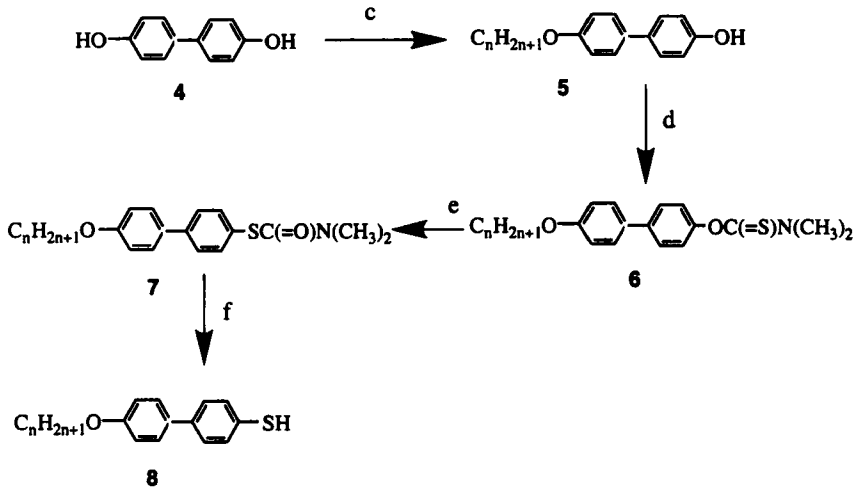

c) C_nH_{2n+1}-Br, KOH, EtOH

d) $(CH_3)_2N(=S)Cl$, DMF, DDO

e) Δ (250°C)

f) KOH, H_2O, ethylene glycol

SCHEME 3 Synthesis of 4-alkyloxy-4′-mercaptobiphenyl

III MESOMORPHIC PROPERTIES

The phase sequences for the whole chiral thiobenzoate series were determined both by Differential Scanning Calorimetry and by optical microscopy. We used an Olympus BX 60 microscope equipped with a Mettler FP5 hot stage for optical observation, and a Perkin-Elmer DSC7 for the calorimetric study. The mesophases identification was carried out by observing the microscopic textures of the materials. Ferroelectric SmC^* mesophase were further characterized by electro-optical measurements.

DSC measurements were performed with various heating and cooling rates (from 0.2 to 5 °C/min). Representative DSC thermograms on heating for compounds n=7 and n=12 are respectively given in figure 1a and figure 1b. The phase sequence, their corresponding phase transition temperatures and enthalpies

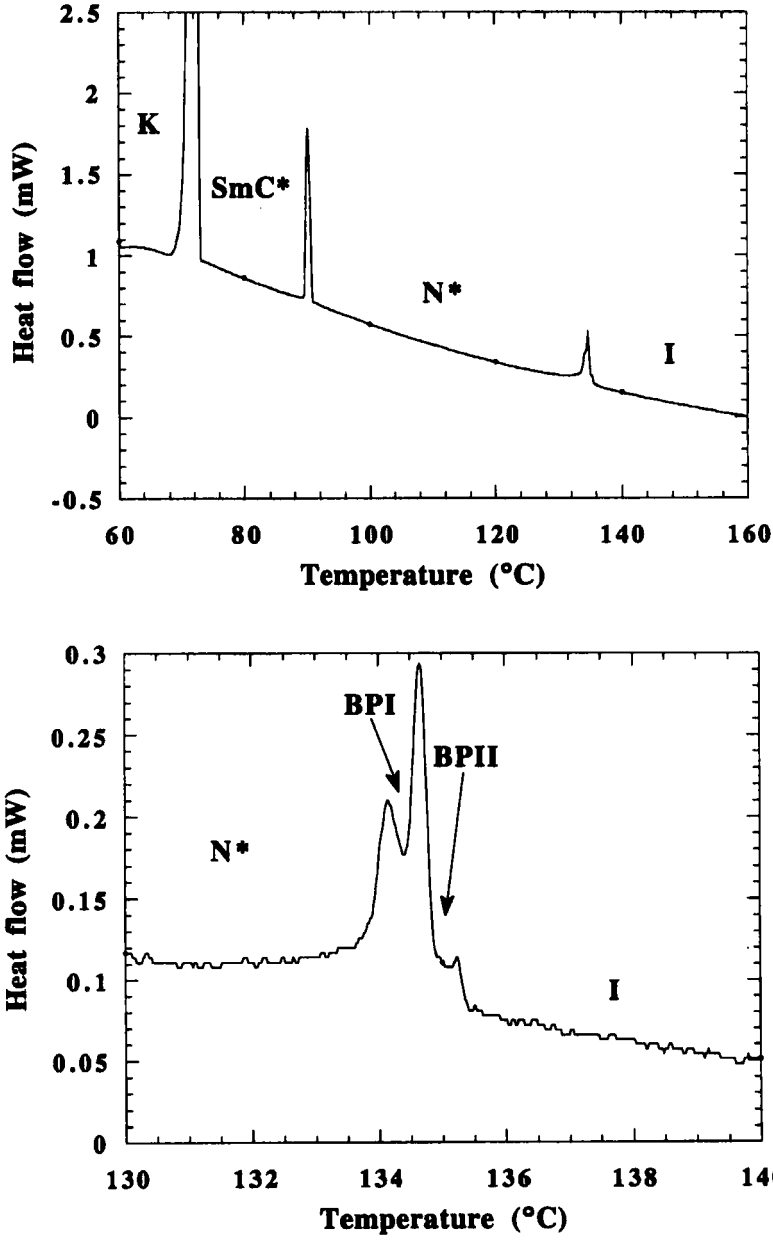

FIGURE 1 (a) DSC thermogram for the heptyloxy derivative on heating at 2°C/min. (b) Enlargement of the DSC thermogram in the temperature range of the BP mesophases for the heptyloxy derivative (heating rate 1°C/min)

are summarized in table I: all the compounds exhibit SmC*, N*, and two BP mesophases. The phase transitions N*-BPI, BPI-BPII and BPII-Isotropic are very close to each other. That is the reason why the enthalpies of each one are difficult to determine. Thus, the enthalpies for the corresponding three overlapped peaks are added together and the BP mesophases are not reported in the table I.

TABLE I Transition temperatures (°C) and enthapies (KJ/mol) in italic according to DSC (on heating at 2°C/min)

n	*K*		*SmC**		*N**		*I*
7	•	72.1	•	90.2	•	134.7	•
		29.3		*2.2*		*1.1*	
8	•	65.8	•	98.7	•	133	•
		23.8		*2.3*		*1.5*	
9	•	56.8	•	103.5	•	131.4	•
		31.5		*2.6*		*1.6*	
10	•	68.6	•	106.4	•	129.6	•
		35.6		*2.7*		*1.6*	
11	•	56.5	•	106.1	•	123.9	•
		20.9		*2.8*		*1.4*	
12	•	61.3	•	106.1	•	122.2	•
		23.5		*3.4*		*1.4*	

A phase diagram as a function of the alkoxy chain length is plotted in figure 2. The transition lines corresponding to the BP mesophases are not taken into account. The N* phase temperature range is greater for n=7 and decreases regularly with n; while the SmC* mesophase range increases on average with n.

The peak shape corresponding to the SmC*-N* phase transition looks like two overlapped peaks; as if there is an intermediate mesophase between the SmC* and the N* mesophase. This phenomenon is particularly visible on the dodecyloxy derivative (see figure 3) where the resolution of the two peaks is good. This behaviour suggests there is probably a TGB or N_L* phase between the N* and SmC* phase. Nevertheless, the optical observation of the texture in various orientations (free surface drops, homeotropic prismatic sample or planar sample) doesn't allow us to distinguish an other mesophase in between the SmC* and N* mesophase. Further investigations in the range of the SmC*-N* transition are currently in progress with our new photothermal method [7]. This point will be also clarified by a high resolution calorimetric study.

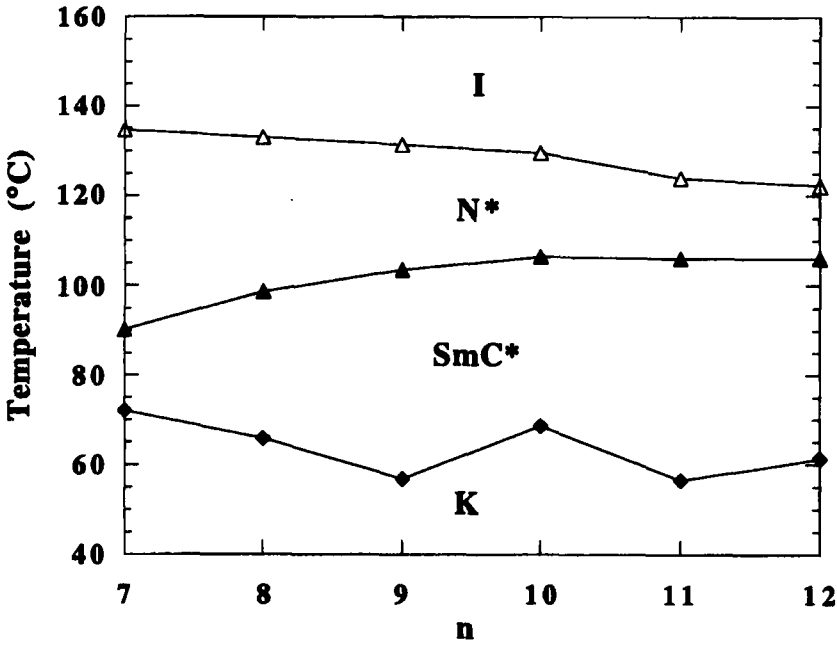

FIGURE 2 Phase behaviour of the series as a function of the alkoxy chain length. The transition lines corresponding to the BP mesophases are not taken into account

IV ELECTRO-OPTICAL PROPERTIES

1°) Samples preparation

The investigation of the electro-optical properties have to be performed in the so-called "bookshelf geometry" [3] where the molecules have to be parallel to the glass plates (planar alignment). The standard way to achieve planar alignment is to use a rubbed polymer on the glass substrate. The quality of the orientation depends both on the interactions between the LC molecules and the polymer, and on the macroscopic structure of the liquid crystal phase (N^*, SmA, SmC^*...) [8]. In our case, neither the commercial nor the "home made" cells give rise to a good orientation quality in the SmC^* phase. In both cases the alignment quality is good in the N^* phase, but the alignment is abruptly destroyed at the N^*- SmC^* phase transition. The figure 4 shows the N^*-SmC^* phase transition on cooling; the grey-blue island are planar N^* area while the granular texture are the SmC^* phase. Moreover, the optical texture of the ferroelectric phase seems to be com-

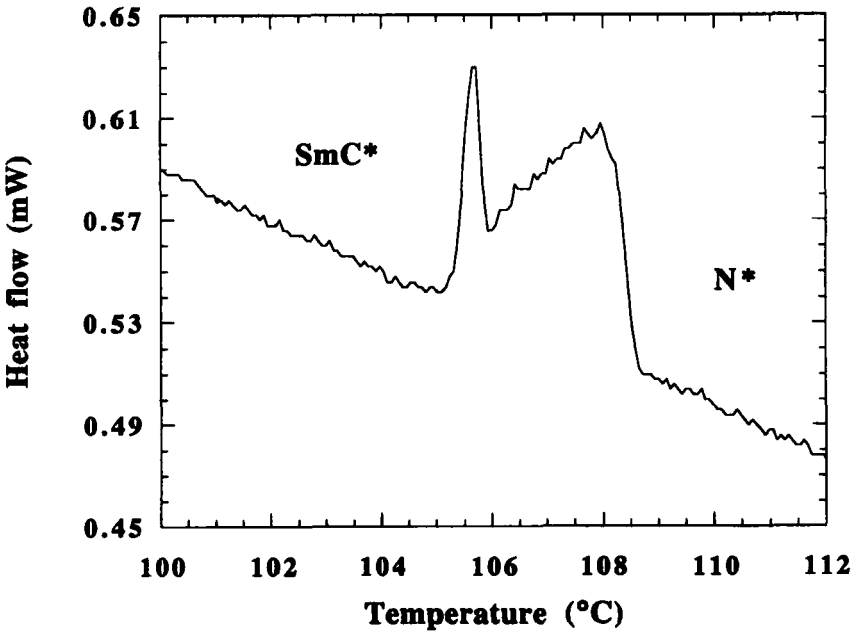

FIGURE 3 DSC thermogram of the SmC^*-N^* phase transition for the dodecyloxy derivative on heating at 0.2°C/min

pletely independent of the surface coating chosen: planar or homeotropic. Indeed, even if we use a surface coating intended for induce an homeotropic alignment (molecules normal to the substrate), like from silanization [9, 10], we obtain the same texture as for planar alignment. The only way we have found to achieve a relatively good planar geometry is to apply a strong alternative electric field. The results are strongly frequency dependent: according to the frequency and also the wave shape (triangle or square) of the applied signal the quality of the alignment can be improved or completely destroyed. The best frequency range is in between 130 and 200Hz, with a triangular wave and under a field value of about 10V/μm. Note that these values of field and frequency are strongly temperature dependent. This dependence is probably linked to the variations of viscosity on the large SmC^* phase range (~40°C). The viscosity variations probably explain the difference of the alignment stability when the electric field is switched off. Indeed, when the field is switch off at high temperature in the SmC^*phase, the planar alignment instantaneously vanishes (see figure 5a). While, at low temperature, a relatively good planar alignment remains after the field is switched off (see figure 5b). This lost of alignment at high temperature in

SmC^* phase is characteristic of the series. An other characteristic of all compounds is their ability to form a mosaic of planar domains [11, 12] (see figure 6). The appearance of these domains is directly linked to the value of the tilt angle at the N^*-SmC^* phase transition. We have found this ability to form a mosaic pattern on all the compounds with two orientations of the smectic layer approximately at right angles; i.e. twice the tilt angle. Each mosaic domain is separated from the next one by a so-called "incoherent wall" [13]; the shape and size of the domains mainly depend on the frequency of the field applied to the sample.

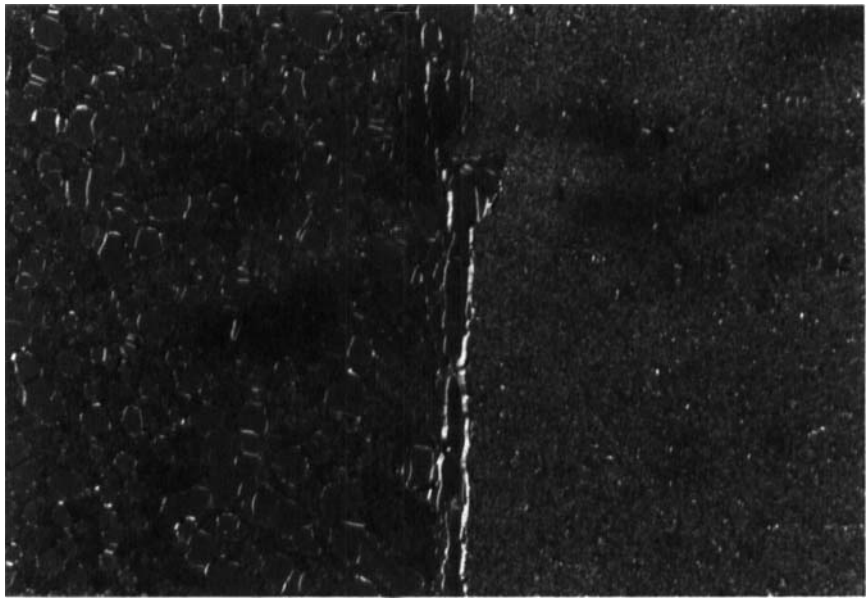

FIGURE 4 The N^*-SmC^* phase transition on cooling in a planar sample coated with polyvinyl alcohol. The blue colour corresponds to the N^* phase in planar geometry, and the granular texture to the SmC^* phase (magnification of 100 in transmission). The slight difference of colour between the right and left side on the photo is due to the presence of the ITO coating (See Color Plate VI at the back of this issue)

2°) Electro-optical measurements

We have investigated the electro-optical properties of the complete series. The physical characteristics (spontaneous polarization, molecular tilt angle, and electric response time) exhibit very weak variations versus the aliphatic chain length; that is the reason why we only present the detailed study for n=7, 10 and 12 compounds.

The temperature dependence of the physical characteristics in the ferroelectric phase for the n=7; 10 and 12 compounds is studied in a 5-μm-thick commercial

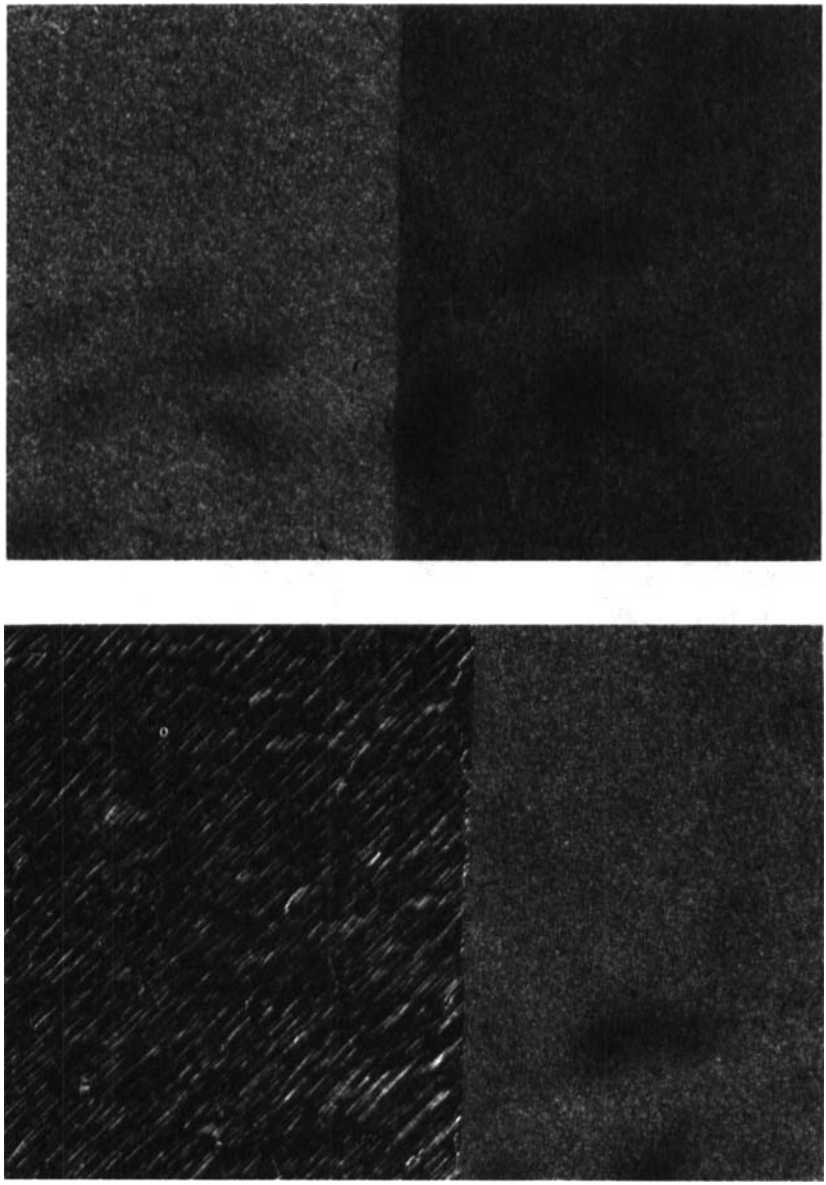

FIGURE 5 (a) Texture observed at 102.5°C in the SmC^* phase of the n=11 compound after switching off the electric field (magnification of 100 in transmission). The electric field has been applied on the bright side of the photograph. (b) Texture observed at 86°C in the SmC^* phase of the n=11 compound after switching off the electric field (magnification of 100 in transmission). The planar alignment remains (See Color Plate VII at the back of this issue)

cells (from Linkam, U. K.). Each cell thickness was checked by an interference method using a 270M-Jobin-Yvon-spectrometer (here the cells thickness varies from 4.8 μm to 5 μm). A classical set-up [14] composed of an HP-33120-A wave form generator, an "home made" amplifier and an HP-54645-A oscilloscope is used for the electro-optical measurement. The sample is placed in a Mettler hot stage (the temperature accuracy is 0.1°C) fixed under an Olympus BX 60 microscope in order to check the optical texture during electro-optical measurement.

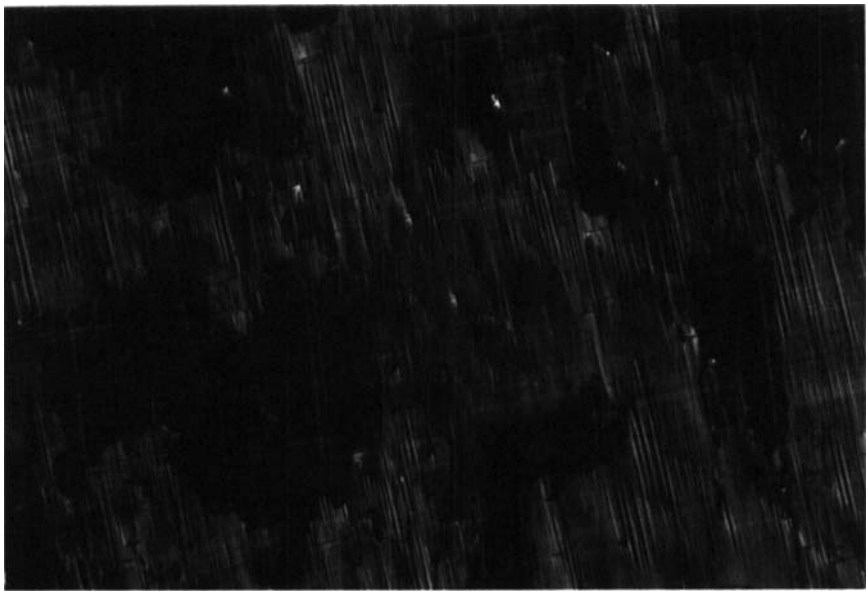

FIGURE 6 Texture observed at 75°C in the SmC* phase of the n=7 compound after switching off the electric field (magnification of 100 in transmission). Note these domains also exist under electric field (See Color Plate VIII at the back of this issue)

The polarization measurements were performed upon heating in the ferroelectric phase. After the whole alignment process, the evolution of the polarization versus electric field is plotted at low temperature in order to determine the field value required to reach the polarization saturation. The saturation was only obtained for very strong field values between 8 and 13V/μm according to the chain length and the temperature (see figure 7). Figure 8 shows the evolution of the polarization versus temperature for the n=7, 10 and 12 compounds. The polarization is almost constant in the SmC* temperature range and exhibits very weak variations with the chain length, 40nC/cm^2 for n=7, and 45nC/cm^2 for n=10 and n=12. The abrupt decreases of the polarization on about 3°C at high temperature is due to the increase of N* domains in the SmC* phase. In figure 8

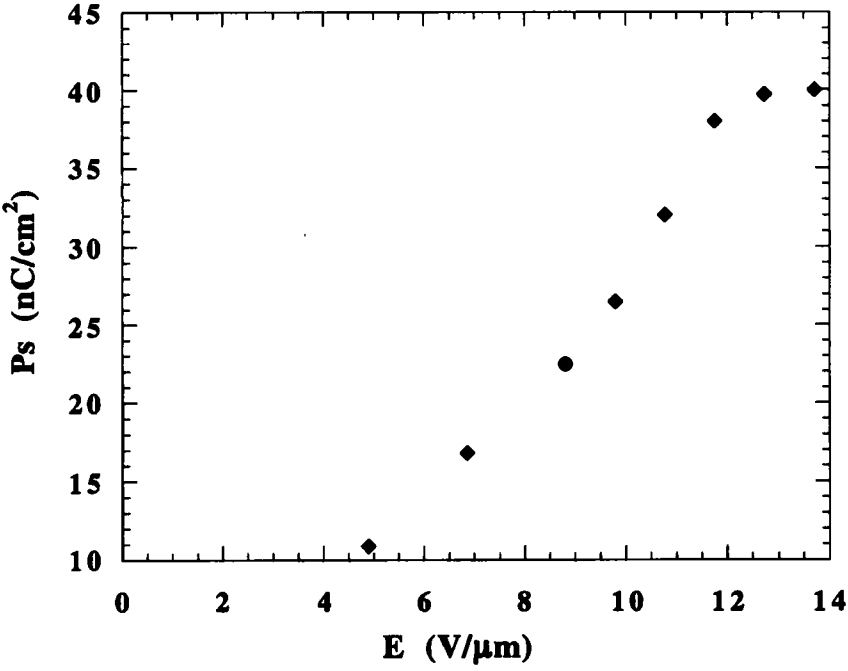

FIGURE 7 Evolution of the polarization versus the electric field for the n=12 compound at 66°C (the measurements were done under triangular wave; v=180Hz)

the arrows show the temperature of appearance of the N^* domains; above this temperature the polarization values decrease abruptly because of the increase of N^* domains in the sample (dotted line). In this biphasic temperature range the area of the SmC^* domains is electric field dependent [11].

The electric response time is defined as the time necessary to reach the maximum of the polarization peak under square waves. The temperature evolution of this time informs about the viscosity of the material (τ is proportional to γ/PE, τ: electric response time; γ rotational viscosity; P: spontaneous polarization; E electric field). Figure 9 shows a typical plot of the temperature dependence of the electric response time (n=12 compound, under an alternative electric field of 8V/μm); τ varies from 136 μs at low temperature (66°C) to 41 μs a few degrees below the SmC^*-N^* phase transition. The slight increase and then decrease between 105°C and 108°C corresponds to the biphasic temperature range (SmC^*+N^*) where the existence of the SmC^* phase is field induced (this part of the graph is plotted in dotted lines). On this series τ decreases with the chain length (minimum value of about 63 μs for n=7).

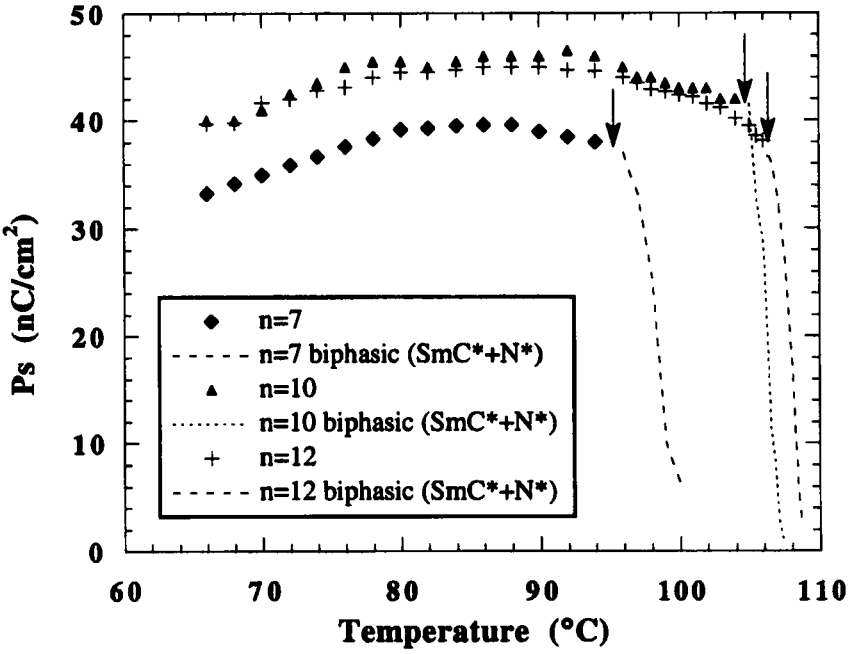

FIGURE 8 Polarization versus temperature for n=7, 10 and 12 compounds. The arrows show the temperature of appearance of the N^* domains. The polarization values in the biphasic temperature range (SmC^*+N^*) are plotted in dotted lines. The field values vary from 10 to 13V/μm following the chain length; ν=180Hz

The apparent tilt angle was estimated using the reversal field method; in this case the accuracy of the measurement is estimated at only + 1.5°C because of the apparent tilt value (θ) of 45°. Indeed, with such a tilt values it is quite impossible to know if we measured 2θ or (2π-θ), all the more that the tilt angle is quasi temperature independent. For all compounds, we have estimated the tilt angle variation at less than 2° on the ferroelectric temperature range. This is the reason why we don't report the plot of the tilt angle versus temperature.

V HELICAL PITCH MEASUREMENTS

Helical pitch measurement on the N^* and SmC^* phases were performed by the well known Grandjean-Cano (GC) method using small angle prismatic cells (about 0.5°). The alignment in the prismatic sample has to be planar in the N^* phase and pseudo-homeotropic in the SmC^* phase [15]. As already mentioned

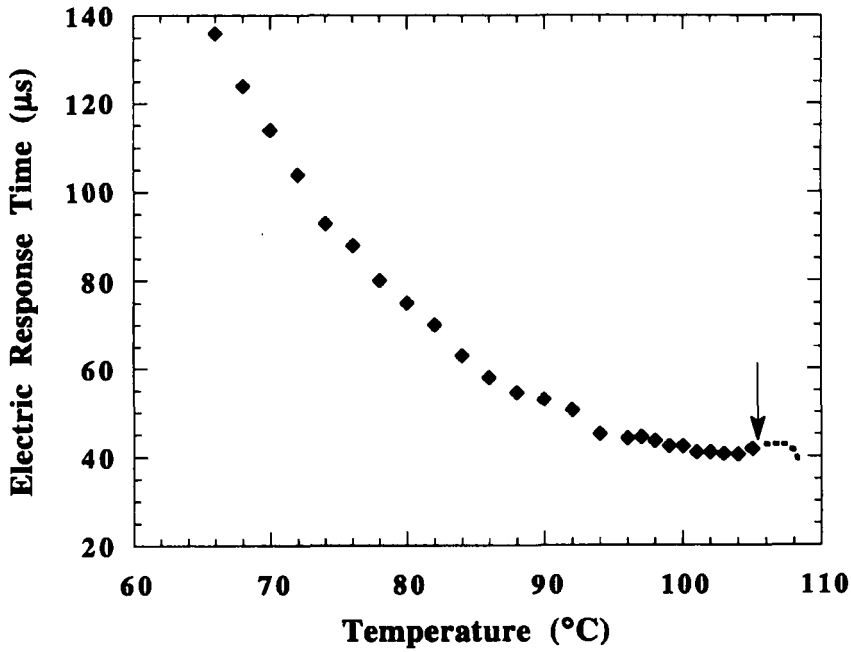

FIGURE 9 Electric response time versus temperature for n=12 compound (Electric field value of 8V/μm; ν=180Hz). The arrow shows the temperature of appearance of the N^* phase; in the biphasic temperature range (SmC^*+N^*) the electric response time is plotted in dotted lines

above, it was easy to obtain planar geometry in the N^* phase by appropriate coating; thus the helical pitch was relatively easily measured in this phase. In the N^* phase the selective reflection of the light could be analysed with a 270M-Jobin-Yvon-spectrometer [16] specially adapted on the microscope.

The pitch values plotted in figure 10 corresponds to GC method checked from the selective reflection of light (λ=np; where λ is the reflected wavelength, n the average refractive index ($n \approx 1.5$) and p the pitch value). The both methods are in very good agreement in the N^* phase.

Concerning the SmC^* phase, the measurements are not convenient because of the weak ability of this phase to align whatever in homeotropic geometry or in planar geometry. In the pseudo-homeotropic orientation the smectic layers are roughly parallel to the substrate and the angular position of the molecules on the smectic cone is fixed on the two glass plates. The poor orientation quality we have obtained in prismatic sample gives sometimes inaccurate values. The number of GC steps available vary from one to five following the compounds; but the results can be check by analysing also the light selectively reflected by

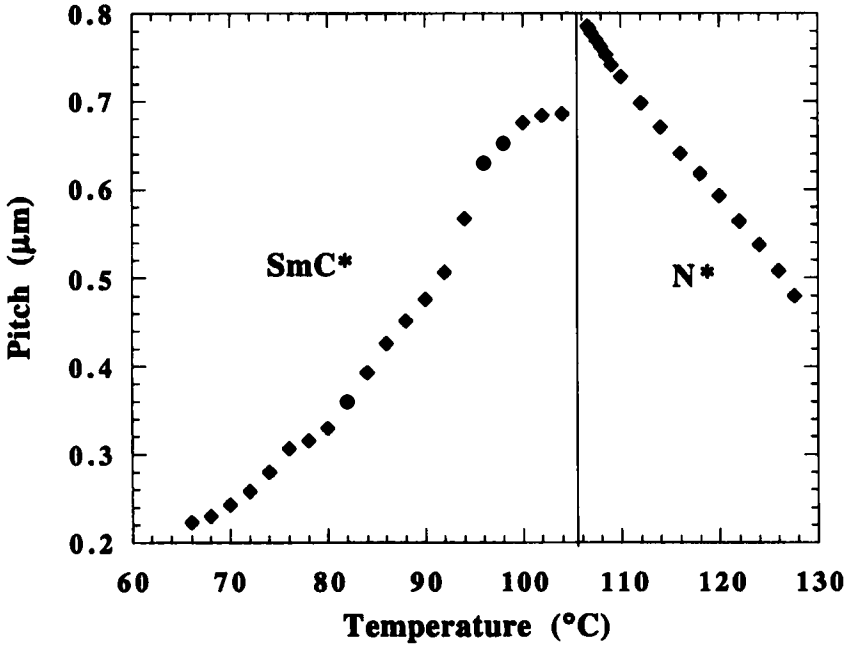

FIGURE 10 Helical pitch versus temperature in the SmC^* and N^* phases for n=10 compound

free surface drops. The drops are deposited on a glass slide coated with silane [9]. The pitch is calculated from the wave length of the light reflected with λ=np if the pitch helix is larger than 0.3 µm and λ=2 np when the values are smaller than 0.3 µm (this limit of 0.3 µm is fixed by sensitivity of the spectrometer).

For n=10 compound, at low temperature in the SmC^* phase, the pitch is very short (0.22 µm at 66°C); the pitch rapidly increases with temperature up to 0.69 µm at 104°C just below the N^* phase (see figure 10). The set of the compounds exhibits approximately the same pitch range and behaviour; for example the pitch varies from 0.12 µm at 60°C to 0.56 µm at 104°C in the SmC^*phase and from 0.7 µm at 105.6°C to 0.435 µm at 130.2°C in the N^* phase for the n=9 compound. The pitch values slightly increase with the aliphatic chain length both in SmC^* and N^* phases.

VI CONCLUSION

The new chiral series with a thiobenzoate core described in this paper displays interesting ferroelectric properties. Indeed, all the compounds exhibit the

N^*-SmC^* phase transition and consequently the molecular tilt angle values are very high (45°).

Moreover, the tilt angle and polarization values are quasi temperature independent. The polarisation values exhibit very weak variation with the chain length (about 40nC/cm^2 for n=7 and 45nC/cm^2 for n=12). The helical structure study has shown a strong twist in the SmC^* phase. In this phase, for the n=9 compound the helical pitch varies from 0.12 μm at low temperature and 0.56 μm just below the SmC^*-N^*Phase transition. Such pitch values are rather unusual for the ferroelectric phase and are incompatible with the realization of Surface Stabilized Ferroelectric Liquid crystal (SSFLC) cell or "Patel cell". Therefore, the realization of mixture are in progress to increase the pitch without change the polarization and the tilt angle values.

On the other hand, this study shows that neither the homeotropic geometry nor the planar geometry seem to be favoured by a tilt angle of 45° with in addition a short helical pitch.

VII EXPERIMENTAL

The infrared spectra were recorded on a Perkin Elmer 783 spectrophotometer and the NMR spectra on a Bruker HW200 MHz spectrometer

(S)-4-(1-methylheptyloxy)benzoic acid (3)

To a cooled solution in a ice bath of ethyl 4-hydroxybenzoate **1** (3.32 g; 0.02 mol), (R)-2-octanol (2.6 g; 0.02 mol), triphenylphosphine (TPP) (5.26 g, 0.02 mol) in 50 ml of CH_2Cl_2 was added dropwise diethyl azodicarboxylate (DEAD) (1.48 g, 0.02 mol) over 15 min. The solution was stirred at room temperature for two hours, filtered and the filtrate was evaporated. The residue was chromatographied on silicagel with a mixture heptane-ethyl acetate (8/2) as eluent. The intermediate ester **2** was obtained and then saponified with KOH (3.36 g) in EtOH under reflux for 3 hrs. The solvent was evaporated and the solid was hydrolyzed with concentrated HCl on ice. The acid was filtered and recrystallized from absolute ethanol. Yield: 3.6 g (63%)

IR: λ_{max} cm^{-1} (nujol), 2594, 2850, 1680, 1610, 1285, 1218, 850.

4-octyloxy-4'-hydroxybiphenyl (5)

To a solution of biphenol (18.6 g, 0.1 mol), KOH (2.8 g, 0.05 mol) in 350 ml EtOH, a solution of 1-bromooctane (9.7 g, 0.05 mol) in 100 ml of EtOH was

added dropwise. The mixture was refluxed for 4 hrs.. After cooling to room temperature, the solvent was evaporated and the residue was treated with water. The solid was filtered and recrystallized from ethanol. After filtration, the desired material is contamined by the diether which was eliminated by treatment with hot heptane. Yield: 8 g (57%)

m. p= 151°C

^{1}H NMR ($CDCl_3$): d (ppm): 0.88 (t, 6H, $2CH_3$), 1.24 (m, 10H, $5CH_2$), 1.35 (d, 3H, CH_3-CH^*), 1.6–1.8 (m, 4H, $2CH_2$), 4.1 (t, 2H, OCH_2), 5.2 (m, 1H, CH-CH_3), 6.9 (d, 2H arom.), 7.2–7.4 (m, 4H arom.), 8 (m, 6H arom.). IR: n_{max} cm^{-1} (nujol), 2594, 2850, 1610, 1285, 1218, 850.

o-4-decyloxybiphenylyl N,N-dimethylthiocarbamate (6)

To a solution of **5** (7.8 g, 0.024 mol) in anhydrous DMF (50 mL) were added diazo-1,4-dicyclo-(2,2,2)octane (DDO) (4.2 g, 0.0375 mol) and N,N-dimethylthiocarbamoyl chloride (4.6 g, 0.0375 mol). The solution was stirred at room temperature for 3 hrs and was heated at 80°C for 1 hr. After cooling to room temperature, it was hydrolyzed with crushed ice, extracted with chloroform. The organic phase was washed with NaOH solution (5%) then HCl solution (10%) and finally with water until neutrality. It was dried over anhydrous sodium sulphate, the solvent was evaporated and the solid was recrystallized from absolute ethanol. Yield: 5.9 g (62%)

m. p=124°C

^{1}H NMR ($CDCl_3$): d (ppm): 0.88 (t, 3H, CH_3), 1.24 (m, 10H, $5CH_2$), 1.6–1.8 (m, 2H, CH_2), 3.3–3.5 (d, 6H, $2CH_3$), 4.1 (t, 2H, OCH_2), 6.9–7.2 (2d, 4H arom.), 7.5–7.7 (2d, 4H arom.).

IR: λ_{max} cm^{-1} (nujol), 2594, 2850, 1610, 1285, 1218, 850.

S-4-octyloxybiphenylyl N,N-dimethylcarbamate (7)

Compound **6** (5 g) is heated in an oil bath at 250°C for 6 hrs. After cooling to room temperature, the desired material is purified by chromatography on silicagel with heptane-ethyl acetate (75/25) mixture as eluent. Yield: 2.1 g (44%) m. p=95°C

^{1}H NMR ($CDCl_3$): d (ppm): 0.88 (t, 3H, CH_3), 1.24 (m, 10H, $5CH_2$), 1.7–1.9 (m, 2H, CH_2), 3.1 (s, 6H, $2CH_3$), 4.1 (t, 2H, OCH_2), 6.9–7.6 (m, 8H arom.).

IR: λ_{max} cm^{-1} (nujol), 2996, 2850, 1680, 1285, 1218, 850.

4-octyloxy-4'-mercaptobiphenyl (8)

In a solution of 1.4 g KOH in 3 ml H_2O and 25 ml ethyleneglycol was added compound **7** (2.1 g; 0.005 mol). The mixture was heated to reflux for 1 hr. After cooling to room temperature, it was hydrolyzed with diluted HCl and crushed ice. The organic compound was extracted with chloroform and the organic phase was washed with water and dried over anhydrous Na_2SO_4. The solvent was evaporated and the residue was recrystallized from a minimum of absolute ethanol. Yield: 1.1 g (78%)

m. p=113°C

^{1}H NMR ($CDCl_3$): d (ppm): 0.88 (t, 3H, CH_3), 1.24 (m, 10H, $5CH_2$), 1.6–1.8 (m, 2H, CH_2), 3.5 (s, 1H, SH), 4.1 (t, 2H, OCH_2), 6.9–7.6 (m, 8H arom.).

IR: λ_{max} cm^{-1} (nujol), 2994, 2850, 2550, 1600, 1285, 1218, 850.

S-4-octyloxybiphenylyl (S)-4-[1-methylheptyloxy]benzoate

(**I**, n=10) Chiral benzoic acid **3** (0.25 g; 0.1 mmol) was added to a solution of **8** (0.34 g; 0.1 mmol), DCC (0.21 g; 0.1 mmol), DMAP (0.01 g) in 5 ml of CH_2Cl_2. The mixture was stirred at room temperature overnight. After filtration, the solvent was evaporated, the solid was chromatographied over silicagel with toluene as eluent. Yield: 0.34 g (66%)

^{1}H NMR ($CDCl_3$): d (ppm): 0.88 (t, 6H, $2CH_3$), 1.24 (m, 18H, $9CH_2$), 1.35 (d, 3H, CH_3-CH^*), 1.6–1.8 (m, 4H, $2CH_2$), 4.1 (t, 2H, OCH_2), 5.2 (m, 1H, CH-CH_3), 6.9 (d, 2H arom.), 7.2–7.4 (m, 4H arom.), 8 (m, 6H arom.). IR: $\lambda_{max}cm^{-1}$ (nujol), 2994, 2850, 1730, 1610, 1285, 1218, 850.

References

[1] F. Tournilhac, L. M. Blinov, J. Simon and S. V. Yablonsky, Nature, **359**, 621 (1992).

[2] T. Niori, T. Sekine, J. Watanabe, T. Furukawa and H. Takezoe, J. Mater. Chem., **6** (7), 1231 (1996).

[3] N. Clark and S. T. Lagerwall, Appl. Phys. Lett., **36**, 11, 899 (1980).

[4] P. Cluzeau, P. Poulin, G. Joly and H. T. Nguyen, 9ème Colloque d'Expression Française sur les Cristaux Liquides, Oral, Hammamet, Tunisie (1999).

[5] J. S. Patel, Appl. Phys. Lett., **60**, 280 (1991).

[6] J.L. Montéro, N. Bello-Roufai, A. Leydet, G. Dewynter, T.Y. N'Guessan, F. Winternitz, Bull. Soc. Chim. France, **2**, 302 (1987).

[7] M. Ismaili, A. Anakkar, G. Joly, N. Isaert, and H. T. Nguyen, Phys. Rev. E, **61**, 519 (2000).

[8] P. Martinot-Lagarde, S. Forget, E. Raspaud, D. Stoenescu, E. Polossat, I. Dozov, P. Auroy and P. Ramdanne, 9ème Colloque d'Expression Française sur les Cristaux Liquides, Oral, Hammamet, Tunisie (1999).

[9] J. B. Brzoska, N. Shahidzadeh and F. Rondelez, Nature, **360**, 719 (1992).

[10] M. P. Valignat, S. Villette, J. Li, R. Barberi, R. Bartolino, E. Dubois-violette, and A. M. Cazabat, Phys. Rev. Lett., **77**, 10, 1994 (1996).

[11] G. Andersson, K. Flatischler, L. Komitov, S. T. Lagerwall, K. Skarp and B. Stebler, Ferroelectrics, **113**, 361 (1991).

[12] T. P. Rieker, N. A. Clark and C. R. Safinia, Ferroelectrics, **113**, 245 (1991).

[13] M. Brunet, L. Lejcek, L. Navailles, submitted to Ferroelectrics.
[14] L. Dupont, M. Glogarova, J. P. Marcerou, H. T. Nguyen and C. Destrade, J. Phys. II, Fr. 1, 831 (1991).
[15] M. Brunet and N. Isaert, Ferroelectrics, 84, 25 (1988).
[16] V. Faye, L. Detre, J. C. Rouillon, V. Laux, N. Isaert and H. T. Nguyen, Liq. Cryst., **24**, 5, 747 (1998).